

Measurement of changes in concentrations of biological solutions using a Rayleigh interferometer

YC Chen and S. J. Kirkpatrick and S. A. Prah

ECE Dept., Oregon Health & Science University, Portland, OR

Sept. 25, 2002

ABSTRACT

A Rayleigh interferometer was constructed to measure changes of concentrations in the biological solutions. With the stability tests, our Rayleigh interferometer system showed its insensitivity to environment vibrations and with the second compensating cuvette, effects on the refractive index changes other than the concentration changes of molecules in the sample solution could be compensated. A thin glass plate was inserted in the beam path and rotated to vary the optical path length to test the sensitivity of the system. With this glass plate, the detectable optical path differences of the system was $\Delta(n\ell) = 7$ nm. Finally, the concentration of sucrose solutions were varied to change the refractive index. The refractive index changes by 1.43×10^{-4} for each gram of sucrose per liter at 20 °C. With our system, the sensitivity to sucrose solution was 7 mg/L. Based on this sensitivity this interferometric system can be used to detect concentrations of albumin solutions as low as 0.6 mg/mL.

keywords: Rayleigh interferometer, biological solutions.

1. INTRODUCTION

Optical interferometers are increasingly being used in biochemical sensing applications.¹⁻¹¹ Interferometry offers label-free, real-time, high-sensitivity advantages. Evanescent-wave interferometers detect the adsorption of molecules within the evanescent field. The drawbacks of the evanescent-wave interferometer are in stability and a tedious alignment process. A single light intensity value from the interference signal is measured using a photodetector,^{2, 8, 10} and therefore any fluctuation in laser intensity or coupling efficiency may be misinterpreted as a change in signal. Other problems with evanescent wave interferometers is that the interference pattern may be changed by (1) changes in the refractive index of the waveguide itself, possibly caused by temperature fluctuations, (2) refractive index changes of the analyte solution, (3) non-specific binding at the waveguide surface, or (4) vibration of the environment. An evanescent wave interferometer with a compensating reference arm has been built,^{1, 6-8} but this increases the complexity of the sensor system and the difficulty on the coupling of the light into the single-mode waveguide. This is especially problematic when the limited lifetime of the bioreagents immobilized on the waveguide surface is considered.

To avoid these disadvantages, we built a Rayleigh interferometer. A Rayleigh interferometer, unlike evanescent-wave interferometers, measures the refractive index changes in analyte solutions instead of those in evanescent field thereby avoiding a alignment problems. A Rayleigh interferometer exploits the interferences of two beams that are divided into upper and lower part such that the differences between the upper and lower part of interference pattern, instead of just one single intensity value on the interference pattern, are analyzed so that the external influences mentioned earlier can be canceled out.

The Rayleigh interferometer was first developed to determine the refractive indices of gases in the early 1900's.¹² It is widely adaptable and has been combined with ultracentrifuge techniques to measure molecular weights.^{3, 9} The Rayleigh interferometer can measure the concentration of molecules with high accuracy due to its sensitivity to the refractive index changes. The Rayleigh interferometer is insensitive to vibration of its environment because the phase shift is calculated by comparing the upper part and lower part of the same

Further author information: (Send correspondence to S.A.P.)

S.A.P.: E-mail: prahl@ece.ogi.edu, Telephone: (503) 216-2197, 9205 SW Barnes Rd., Portland, OR 97006, USA

fringe. Any vibration will affect both the upper and lower part of fringes equally. Another advantage is that the degree of the resolution on the changes of the refractive index can be modified by changing the sample path length and the magnification of the fringe patterns. Finally, the two beams can be widely separated as long as the magnification of the cylindrical lens is large enough. This leaves a flexible space for designing two chamber sample holders.

The design and operation of the conventional Rayleigh interferometer generally follow those of figure 1.¹² Light from slit S is collimated by lens L_0 falling on the two slits S_1, S_2 . These two parallel rays pass through the two chambers, and are recombined by the lens L_1 . The fringe patterns are then magnified by a cylindrical lens L_2 . The sample is put in the upper part of the beam, and the glass plate G is displaced into the lower part of the beam to compensate the fringes. The position of G is adjusted such that the upper edge of G meets the lower edge of the sample in a sharp dividing line appearing in the fringe patterns. To compensate for the fringe shift caused by changes in the optical path length, two thin glass plate C_1 and C_2 placed in the upper part of the beams can be rotated until the shift of fringes are realigned. In this system, the alignment of the two compensating glass plates C_1 and C_2 can be tedious. In addition, the use of the rotation of the glass plate to compensate the optical path difference is dependent on the vernier acuity of human's eye.

In this study, minor modifications to the conventional Rayleigh interferometer were made to eliminate the compensating glass plates C_1 and C_2 . The two beams were recombined to form an interference pattern that was magnified by a cylindrical lens with a short focal length. The fringes were formed directly on a CCD camera for visualization and fringe analysis. Samples were placed only in the upper portion of the beams, thereby altering only the upper portion of the fringe pattern. The lower portion of the fringe pattern served as a reference. Small changes in the refractive index of the sample were measured by comparing the upper and lower fringe patterns.

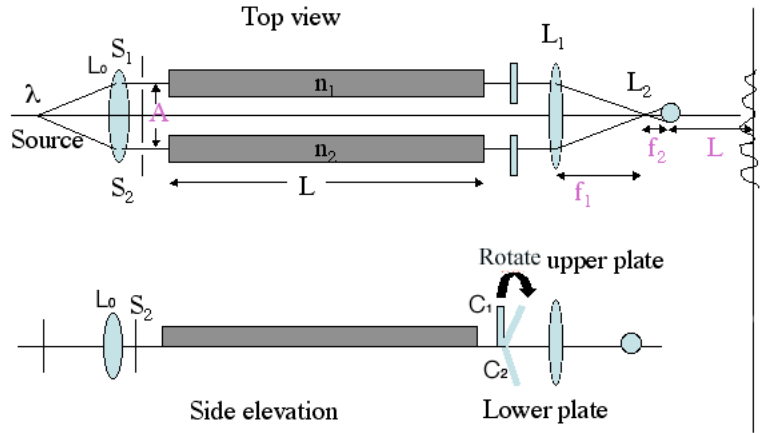


Figure 1. The conventional Rayleigh interferometer¹² First, the light from slit S is collimated by lens L_1 falling on the two slits S_1, S_2 , then the two parallel rays passed through the two chambers, finally recombined by the lens L_2 . The fringe patterns are then magnified by the cylindrical lens.

2. THEORY

Figure 1 shows the geometry of the classic Rayleigh interferometer.¹² Assume the focal lengths of the lenses, L_1 and L_2 , are f_1 and f_2 , the separation of two slits is A , The distance between the lens L_2 and the screen is

L , then the spacing of the interference fringes at screen $X - Y$ plane is

$$\Delta x = \frac{\lambda L f_1}{A f_2} \quad (1)$$

Therefore, the width of the fringes can be adjusted by changing the fraction of f_1 and f_2 .

Assume the irradiances of the two beams are equal to I_0 , then the irradiance of the interference pattern at point x is

$$I(x) = 2I_0 + 2I_0 \cos\left((\vec{K}_1 - \vec{K}_2) \cdot \vec{r} + \Delta\varepsilon\right) = 2I_0 + 2I_0 \cos\left(2\pi \cdot \frac{x}{\Delta x}\right) + \Delta\varepsilon, \quad (2)$$

where \vec{K}_1 and \vec{K}_2 are the propagation vectors of the spherical wavefronts, \vec{r} is the position vector at the point of observation, x , on the screen, and $\Delta\varepsilon$ is the initial phase difference of the two beams from the lens L_2 .¹⁴ The interference pattern is caused by the $(\vec{K}_1 - \vec{K}_2) \cdot \vec{r}$ term, which varies from point to point on the $X - Y$ screen. The fringe pattern will be shifted by varying $\Delta\varepsilon$, which is caused by the optical path length difference $\Delta(OPL)$ of the two beams. The phase shift of fringes shift is

$$\Delta\Phi = \Delta\varepsilon_1 - \Delta\varepsilon_2 = 2\pi \frac{\Delta(OPL)}{\lambda} = 2\pi \frac{\Delta(n\ell)}{\lambda} \quad (3)$$

where ℓ is the path length and n is the refractive index of the media. The two methods used to test the sensitivity of our interferometer system were to change the interaction pathlength of the light ℓ with the media and changing the refractive index of the sample media n .

2.1. Vary the path length (ℓ)

One way to vary ℓ is to rotate a thin glass plate. As shown in figure 2, by rotating the glass plate, not only is the path length in the glass plate changed, but the path length of the light passing through the air is changed. Assume the refractive index of the air is 1 and the refractive index of the glass plate is n , the thickness of the glass plate is d , and the angle of rotation is θ , then changes in the OPL becomes

$$\Delta(OPL) = (\ell_1 + d + \ell_2) - (\ell'_1 + \ell' + \ell'_2) = d \left(\sqrt{n^2 - \sin^2 \theta} - \cos \theta - (n - 1) \right) \quad (4)$$

The phase shift $\Delta\Phi$ can be obtained using equation (3).

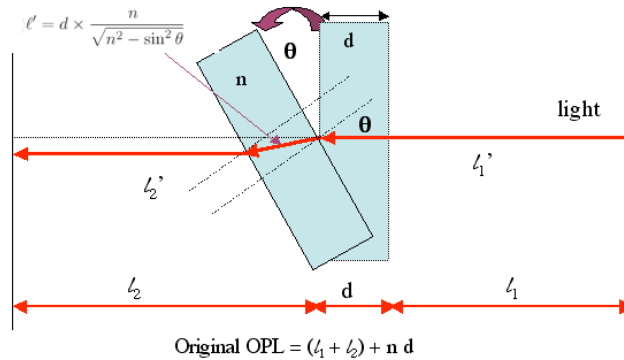


Figure 2: Rotation of the coverslip.

2.2. Vary the index of refraction (n)

When the refractive index of the sample changes from n to n' , the phase shift of the fringes is

$$\Delta\Phi = 2\pi \frac{\ell(n - n')}{\lambda}$$

A simple and reliable way to determine the sensitivity of my system on the refractive index is to measure the refractive index of sucrose solutions of various concentrations. According to the literature,^{1,3,13} a sucrose solution at 20°C causes changes of refractive index of 1.43×10^{-4} for each gram of sucrose added to one liter of water. Therefore, the phase shift with regard to the concentration change (ΔC) is

$$\Delta\Phi = 2\pi \frac{\ell(1.43 \times 10^{-4})\Delta C}{\lambda} \quad (5)$$

3. EXPERIMENTS

The experiments can be divided into four parts. The first was to test the vibration stability of the system, the second evaluated the importance of a second compensating cuvette on stability, the third was to rotate a thin glass plate to vary the pathlength and fourth was to measure the refractive index of sucrose solutions at various concentrations. Interference patterns were recorded with a CCD camera for data analysis. The fringe image was a 640×480 ($x \times y$) pixel picture. To avoid edge effects only the middle 512 pixels (from the 65th to 576th pixel in x direction) of the picture were used. The average of the upper portion of the fringe pattern was taken from the 20th through the 40th pixel (in y direction) of the picture while the average of the lower portion was taken from the 440th through the 460th pixel of the picture. (Please see figure 3.) The Fast Fourier Transform function in Matlab software was used to analyze the frequency components and their phases.

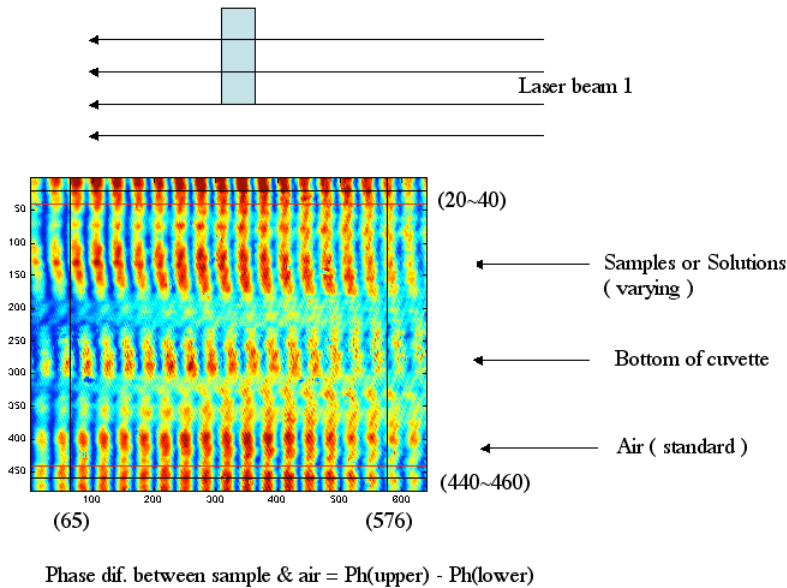


Figure 3: Picture of interference pattern.

3.1. Stability tests

3.1.1. Vibration of surroundings

The experimental setup is illustrated in figure 4. Only one cuvette was used in this experiment. The cuvette was empty. To test the influences of surrounding vibrations, we recorded the fringes every 5 seconds as the door of

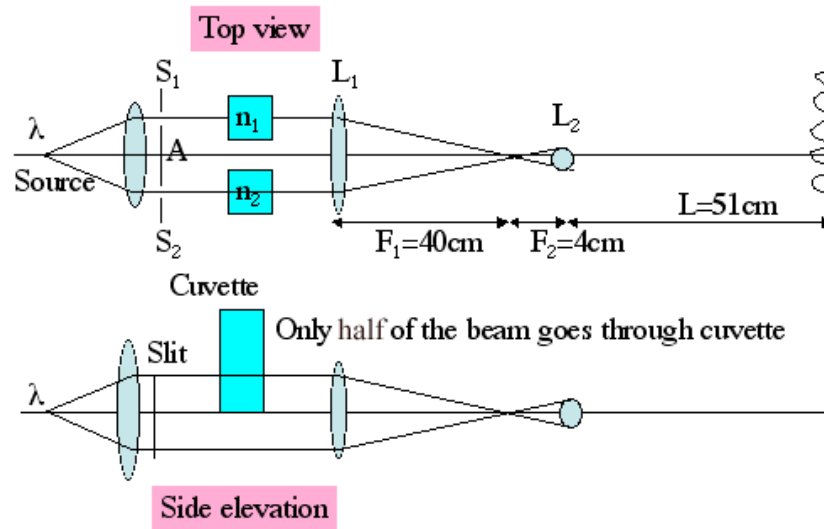


Figure 4: Experiment setup.

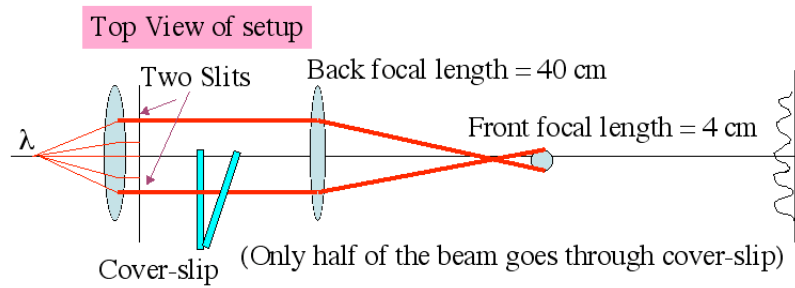


Figure 5: Experimental setup of rotating the coverslip.

the laboratory was opened and closed, as people walked or jumped near the optical table, and following a knock on the optical table. The tests were made on a non-floating optical table (4-leg MELLES GRIOT 070TK021).

3.1.2. Compensation cuvette

This experiment tested the compensation effect of the second cuvette in the second arm. Using the same experimental setup (figure 4), the cuvettes were filled with pure water. The 1×1 cm quartz cuvettes were arranged so that the beam passed through the lower portion of the cuvettes to avoid the meniscus of the solution surface, which contaminates the interference patterns in the image plane. We compared the phase stability when there was only one cuvette set to the upper portion of one beam and when two cuvettes were present.

3.2. Sensitivity tests

3.2.1. Rotating a thin glass plate

This test was to observe the fringe shift versus the rotation of the cover slip. The experimental setup is shown in figure 5. A 0.15 mm coverslip was fixed on a rotational stage and was set at the lower portion of one beam. The images were displayed by a 1×0.75 cm CCD camera with 640 by 480 pixel resolutions. The distance of CCD to the cylindrical lens was adjusted such that there were about 10 fringes shown in the image. The fringes were recorded at rotation angle of $0 - 12^\circ$ both counterclockwise and clockwise. The index of refraction of the cover-slip was measured by Abbé refractometer (ABBE-3L Refractometer 13-964-10, Fisher Scientific).

3.2.2. Sucrose solutions

The experimental setup is the same as figure 4. One cuvette filled with the solution to test was placed in the sample arm, while the other cuvette filled with pure water. This compensated for temperature changes in the solution. The prepared solution was filled into the sample cuvette starting from the lowest concentration. The concentration was increased by adding higher concentration solutions. The compensating cuvette was filled with the same amount of volume of pure water each time. The pipette tip was used to carefully mix the solutions. For each concentration of solution, fringes were recorded every 20 seconds for 1 hour to ensure the solution was totally mixed.

4. RESULTS

4.1. Stability Tests

4.1.1. Vibration of surroundings

The results of vibration test are shown in figure 6. The magenta(middle), blue(bottom) and red(top) circle-curve are respectively represented the phases of upper, lower part of the fringes and the differences ($\Delta\Phi$) of these two parts. For the first 100 seconds when there was nobody moving, the $\Delta\Phi$ was $227 \pm 1^\circ$. The second period when there was someone opening and closing the door, $\Delta\Phi$ was $227 \pm 1^\circ$. The third period when there was again nobody moving, $\Delta\Phi$ was $228 \pm 1^\circ$. The fourth period when there was someone jumping close the optical table, $\Delta\Phi$ was $228 \pm 1^\circ$. Then, nobody was moving around again, $\Delta\Phi$ was $226 \pm 1^\circ$. For the final period right after someone knocked the optical table, $\Delta\Phi$ was $225 \pm 1^\circ$.

4.1.2. Compensating cuvette

The comparison of one-cuvette and two-cuvette experiments is shown in figure 7. The magenta(middle), blue(top) and red(bottom) circle-curve are respectively represented the phases of upper, lower part of the fringes and the differences ($\Delta\Phi$) of these two parts. Phase $\Delta\Phi$ was more stable when there were two cuvettes. The average $\Delta\Phi$ value of one-cuvette test was $-223 \pm 12^\circ$ for 2.5 minutes, while $\Delta\Phi$ value of two-cuvette test was $-307 \pm 1^\circ$ for the last 2.5 minutes.

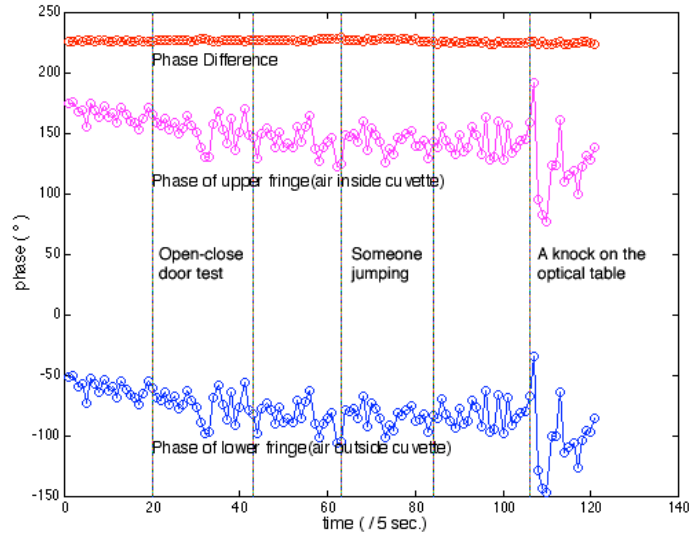


Figure 6. Phase shifts and differences measured in the surrounding-vibration test. The results were divided into 6 testing periods representing no movement, open-close door, no movement, people jumping, no movement and a knock on the optical table respectively. Although the phase of upper and lower fringes varied for more than 50° , the difference between these two remains fairly stable (within 1° deviation).

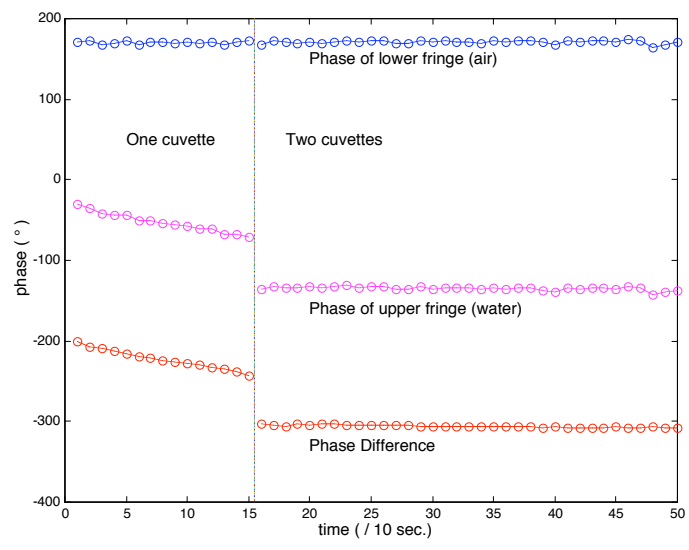


Figure 7. Results of compensating-cuvette experiment. $\Delta\Phi$ of one-cuvette was $-223 \pm 12^\circ$ for 2.5 minutes, while $\Delta\Phi$ of two-cuvette was $-307 \pm 1^\circ$ for the last 2.5 minutes, which is much stabler.

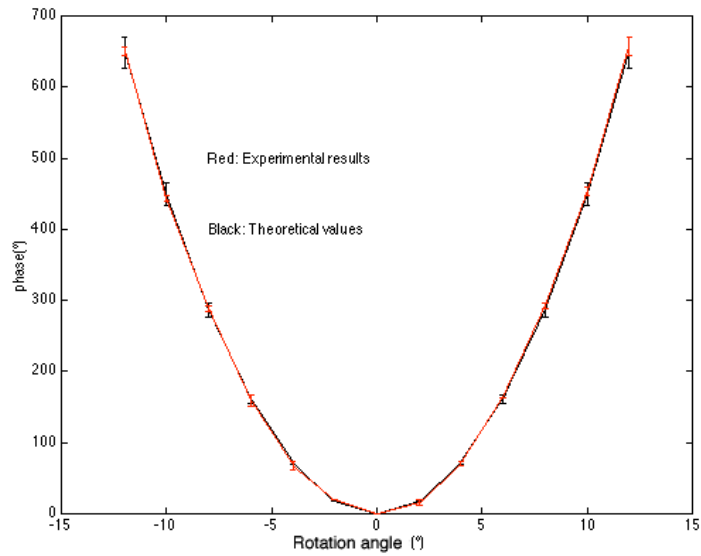


Figure 8. The experimental results (red curve) and the theoretical values (black curve) versus the rotating angles of the coverslip. This shows the experimental results agree with the prediction within the estimated error of the interferometric measurement.

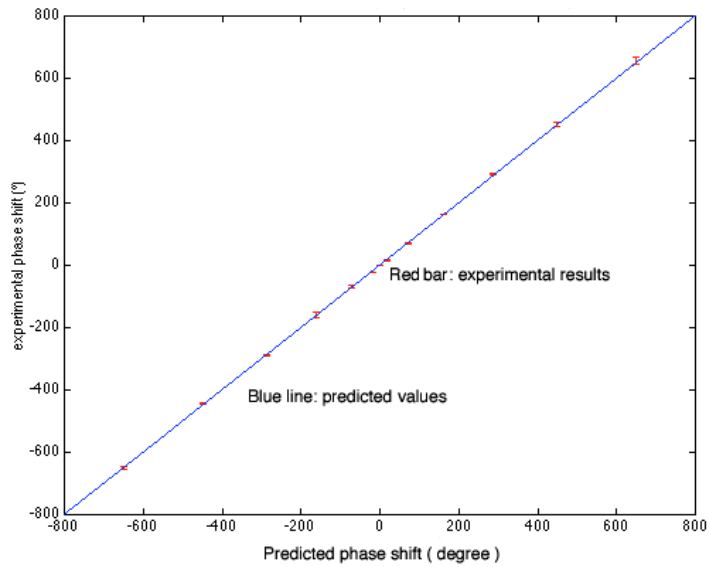


Figure 9. This is a different plot of results of rotation of the coverslip: the experimental results (red bar) versus the predicted values (blue line).

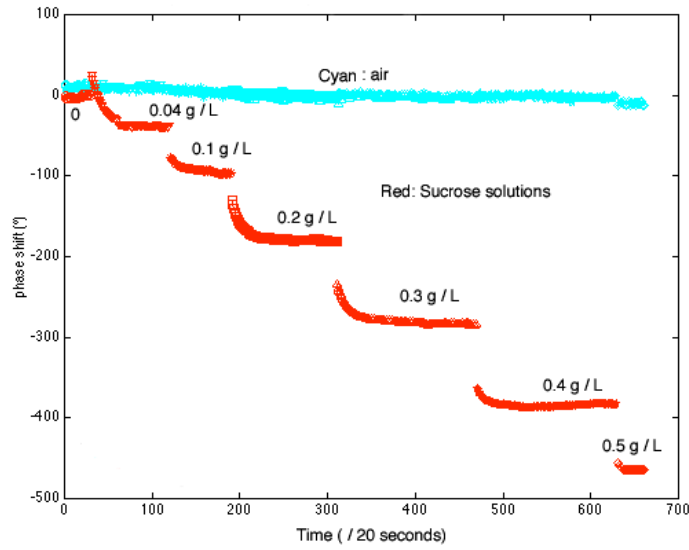


Figure 10. The results of sucrose experiment. Red points are the phase differences as adding the concentrate sucrose solution to the previous solution, while blue points represent the phases of lower fringe (air). As we see, the phase was changing as concentrated sucrose solution was added and then stabilized after a period of time.

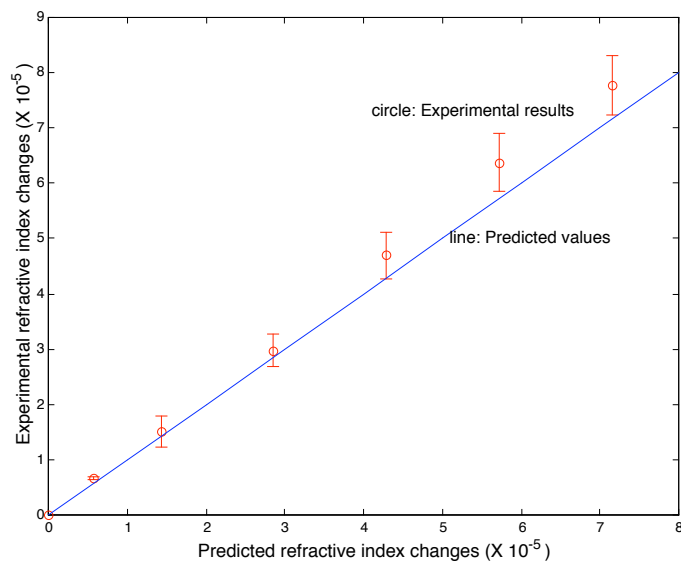


Figure 11. Experimental refractive index results (red bar) versus the predicted refractive index values (blue line). The experimental refractive index changes are greater than the predicted ones. This is probably the result of higher sucrose concentration at the bottom of the cuvette due to gravity.

4.2. Sensitivity Tests

4.2.1. Rotating a thin glass plate

The index of refraction of the cover slip measured by Abbé refractometer is 1.5219 ± 0.0010 . The thickness is 0.15 mm. Figure 8 shows both the experimental and predicted results of the phase shift of the fringes versus the rotation angle of the cover-slip. The experimental fringe shifts versus the predicted fringe shifts is plotted in figure 9.

4.2.2. Sucrose solutions

Figure 10 is the result of phase shifts (in degree) as adding the concentrate sucrose solution to the previous solution. Figure 11 is the plot of the experimental measurement results of refractive index versus the predicted refractive index values.

5. DISCUSSION

5.1. Stability

Figure 6 shows that our system is insensitive to surrounding vibrations. Although the phase of upper and lower fringes varied for more than 50° , the difference between these two remains fairly stable (within 1° deviation). For the compensating-cuvette experiment, figure 7 shows that with two cuvettes in the two beams is more stable. This means the second (compensating) cuvette is able to compensate the changes of refractive index of the solution in the sample cuvette.

5.2. Sensitivity

We used two methods to test the sensitivity of the Rayleigh interferometer. The experiment of rotating a thin glass plate is a good method to test the sensitivity of the system, but is limited by the accuracy of measuring the rotation angle. Figure 9 shows that experimental results agree with the prediction within the estimated error of the interferometric measurement. The errors possibly come from the variation of rotation angles, the variation of thickness of glass plate and the refractive index variation of the glass plate due to the compression by the clip. The sucrose solution experiment (figure 10) suggests that a complete mixing in the solution was important to obtain accurate concentrations and therefore to get an accurate refractive index value. Figure 11 shows that the experimental refractive index changes are greater than the predicted ones. This is probably the result of higher sucrose concentration at the bottom of the cuvette due to gravity.

In conclusion, with the stability tests, we had shown that our Rayleigh interferometer system was insensitive to environment vibrations and that effects on the refractive index changes other than the concentration changes of molecules in the sample solution could be compensated by the second compensating cuvette. With this system, 7 mg/L concentration changes of sucrose solution (equivalent to $\Delta n = 10^{-6}$) can be measured. Based on this sensitivity this interferometric system can be used to detect concentrations of protein solutions as low as 0.6 mg/mL using albumin as an example (albumin solution causes changes of refractive index of 1.74×10^{-6} for each gram added to one liter of water at 24°C).¹⁵

This interferometric system can be used with biological recognition elements to detect the binding of molecules and their counterparts. Compared with the evanescent-wave type interferometers, the production of the thin-layer waveguide and the complicated light-coupling procedure can be avoided in our system. The second cuvette is able to compensate the environmental effects on the samples but does not increase the complexity of the system. The sensitivity of this interferometric sensing system for detecting concentration changes of biological solutions only depends upon the sensitivity of the interferometer to changes of the refractive index, and on how much the refractive index changes with analyte concentration. We have shown that our system can be a robust, sensitive and real-time biochemical sensing device.

REFERENCES

1. A. Brandenburg and R. Krauter and C. Kunzel and M. Stefan and H. Schulte, "Interferometric sensor for detection of surface-bound bioreactions," *Appl. Opt.*, **vol. 39**, pp. 6396–6405, 2000.
2. F. Brosinger and H. Freimuth and M. Lacher and W. Ehrfeld and E. Gedig and A. Katerkamp and F. Spener and K. Cammann, "A label-free affinity sensor with compensation of unspecific protein interaction by a highly sensitive integrated optical Mach-Zehnder interferometer on silicon," *Sensors and Actuators B*, **vol. 44**, pp. 350–355, 1997.
3. D. Bucher and E. G. Richards and W. D. Brown, "Modifications of the Rayleigh Interferometer in the ultracentrifuge for use with Heme and other light-absorbing proteins," *Anal. Biochem.*, **vol. 36**, pp. 368–380, 1970.
4. H. Helmers and P. Greco and R. Rustad and R. Kherrat and G. Bouvier and P. Benech, "Performance of a compact, hybrid optical evanescent-wave sensor for chemical biological applications," *Appl. Opt.*, **vol. 35**, pp. 676–680, 1996.
5. S. Kubitschko and J. Spinke and T. Bruckner and S. Pohl and N. Oranth, "Sensitivity enhancement of optical immunosensors with nanoparticles," *Anal. Biochem.*, **vol. 253**, pp. 112–122, 1997.
6. B. H. Schneider and J. G. Edwards and N. F. Hartman, "Hartman interferometer: versatile integrated optic sensor for label-free, real-time quantification of nucleic acids, proteins, and pathogens," *Clin. Chem.*, **vol. 43**, pp. 1757–1763, 1997.
7. B. H. Schneider and E. L. Dickinson and M. D. Vach and J. V. Hoijer and L. V. Howard, "Highly sensitive optical chip immunoassays in human serum," *Biosen. and Bioelec.*, **vol. 15**, pp. 13–22, 2000.
8. B. H. Schneider and E. L. Dickinson and M. D. Vach and J. V. Hoijer and L. V. Howard, "Optical chip immunoassay for hCG in human whole blood," *Biosen. and Bioelec.*, **vol. 15**, pp. 597–604, 2000.
9. I. Z. Steinberg and H. K. Schachman, "Ultracentrifugation studies with absorption optics. V. analysis of interacting systems involving macromolecules and small molecules," *Biochem.*, **vol. 5**, pp. 3728–3747, 1966.
10. M. Weisser and G. Tovar and S. Mittler-Neher and W. Knoll and F. Brosinger and H. Freimuth and M. Lacher and W. Ehrfeld, "Specific bio-recognition reactions observed with an integrated Mach-Zehnder interferometer," *Biosen. and Bioelec.*, **vol. 14**, pp. 405–411, 1999.
11. C. Worth and B. Goldberg and M. Ruane and S. Unlu, "Surface Desensitization of polarimetric waveguide interferometers," *IEEE J. Quantum Electronics*, **vol. 7**, pp. 874–877, 2001.
12. M. Born and E. Wolf "Principles of Optics," *Cambridge University Press*, 1999.
13. British Sugar Technical Centre, "International Commission for Uniform Methods of Sugar Analysis," *ICUMSA Publications*, 1974.
14. F. L. Pedrotti and L. S. Pedrotti, "Introduction to Optics," *Prentics-Hall International, Inc.*, 1993.
15. T. P. Moffitt and D. A. Baker and S. J. Kirkpatrick and S. A. Prahl, "Mechanical properties of coagulated albumin and failure mechanisms of liver repaired with the use of an argon-beam coagulator with albumin," *J. Biomed. Mater. Resea. Appl. Biomater.*, accepted for publication, 2002.